# Wideband 10-Port MIMO Antenna Array for 5G Metal-Frame Smartphone Applications

**Peng Liu, Yufa Sun\*, Tao Liu, Qing Li, and Xuefeng Wang**

**Abstract**—A wideband 10-port multiple input multiple output (MIMO) antenna array operated below 6 GHz for the fifth generation (5G) metal-frame smartphones is presented and discussed in this paper. The proposed MIMO antenna array element is composed of a microstrip line with a tuning stub and rectangular slot. The size of the rectangular slot is only $15\,\mathrm{mm} \times 2\,\mathrm{mm}$ ($0.211\lambda_0 \times 0.028\lambda_0$, and $\lambda_0$ is the wavelength with the resonance frequency of 4.2 GHz). U-shaped slots on the substrate are used to reduce the mutual coupling between the antenna elements. At the same time, in order to improve the radiation characteristics of the antenna arrays, narrow slits are etched in the metal-frame. The proposed antenna covers 3.3–5.5 GHz ($S_{11} < -6\,\mathrm{dB}$), which is ultra-wide bandwidth for the 5G communications. The proposed MIMO antenna array is fabricated and measured. Results show that in the desired wide frequency band, the proposed antenna array can achieve desirable performances, including antenna isolation better than $-13\,\mathrm{dB}$ with decoupling structures, efficiency, and envelope correlation coefficient (ECC) $< 0.06$. Moreover, radiation pattern, calculated ergodic channel capacity, the user's hand effects and head specific absorption rate (SAR) are also given in the paper. Good agreement between measured and simulated results is obtained, which means that the proposed MIMO array is a good candidate for 5G metal-frame smartphone applications.

## 1. INTRODUCTION

With the great development of modern mobile wireless communication systems, antennas for the fifth generation (5G) of mobile communication have aroused widespread concerns from both academia and industry. It has been acknowledged that massive multiple input multiple output (MIMO) antenna technology is the key point for realizing 5G applications, because it has many advantages for high data rates, low latency, large system capacity, and large-scale device connectivity [1]. This technology uses multiple transmitting and receiving antennas to improve communication quality. It can make full use of space resources and can greatly improve system channel capacity without increasing spectrum resources and antenna transmit power [2, 3]. Conventional $2 \times 2$ MIMO antennas for long term evolution (LTE) communications can no longer afford such high data throughput, so $8 \times 8$ MIMO or even $10 \times 10$ MIMO antenna system is currently necessary [4–6].

Nowadays, research on the frequency bands below 6 GHz (sub-6 GHz) in most countries of the world focuses on LTE band 42 (3.4–3.6 GHz) and LTE band 43 (3.6–3.8 GHz). Besides, 3.5–4.2 GHz, 3.3–3.4/4.8–5.0 GHz, and 3.6–4.2/4.4–4.9 GHz are also included in 5G applications by the United States, China, and Japan, respectively. As a representative of future 5G wireless communications, Table 1 shows the sub-6 GHz bands of some countries. From Table 1, it is shown that different countries have allocated different sub-6 GHz bands ranging from 3.3 GHz to 5 GHz. The above-mentioned frequency bands have been intensively studied in some previous works [7–12]. Note that the 5.0–5.5 GHz, which is part of

**Table 1.** Sub-6 GHz spectrum of some countries.

| Country | Spectrum |
|---------|----------|
| China | 3.3–3.6 GHz/4.8–5.0 GHz |
| America | 2.49–2.69 GHz/3.5–3.7 GHz |
| England | 3.4–3.8 GHz |
| Europe | 3.4–3.8 GHz |
| Japan | 3.6–4.2 GHz/4.4–4.9 GHz |
| France | 3.46–4.8 GHz |
| Italy | 3.6–3.8 GHz |
| Korea | 3.4–3.7 GHz |
| Australia | 3.4–3.7 GHz |
| Germany | 3.4–3.8 GHz |

LTE band 46 (5.150–5.925 GHz), is not adopted in the most countries for a while, but it is considered as an important spectrum for the future development of 5G applications [13, 14].

On the other hand, the metal-frame has gradually become an important part for a smartphone in industrial design, because of their mechanical strength enhancement as well as aesthetic appearance. However, integrating multiple antennas into a metal-frame smartphone can deteriorate the antenna's radiation performance and isolation. Fortunately, etching the slit structures on the metal-frame can effectively solve this problem [15–18]. The application of new decoupling technologies and structures such as substrate integrated waveguide (SIW) and electromagnetic band gap (EBG) has greatly improved the isolation between adjacent antennas [19–21]. In recent years, some multi-band 5G MIMO antenna arrays have been reported for 5G mobile communications, while only a few can integrate metal-frame as a vital component for the smartphones [22–24]. These multi-band antennas have shown good performances in the non-metallic smartphone platform, but these design concepts may not be applicable to mobile phones with metal-frame [25–27]. Therefore, we still need new ideas to resolve the problem of deteriorated antenna performance under metal coverage, especially for 5G MIMO antenna arrays in smartphone applications.

In this paper, a wideband 10-port MIMO antenna array for 5G metal-frame smartphones is proposed. The antenna array can operate in the frequency from 3.3 GHz to 5.5 GHz, which includes almost all sub-6 GHz bands in 5G applications. The antenna array is composed of ten same antenna elements. Each antenna element consists of a microstrip line with a tuning stub and rectangular open slot. At the same time, to reduce mutual coupling, a U-shaped slot is embedded between the two antenna elements at the ground plane. The system circuit board is surrounded by metal-frame with narrow slits, and the side edge metal-frame is directly fed by the microstrip line. A prototype of the antenna is fabricated and measured. Typical results such as $S$ parameters, antenna efficiencies, radiation patterns, and calculated envelope correlation coefficients (ECC) are discussed in the paper. Lastly, the effect of user's hand posture and SAR on the performances of the MIMO antenna array is also simulated.

## 2. DESIGN OF THE PROPOSED ANTENNA ARRAY

### 2.1. Antenna Array Structure

Figure 1 shows the geometry and physical dimensions of the proposed wideband 10-port MIMO antenna array. A 0.8 mm-thick FR4 substrate with a relative permittivity of 4.4 and a loss tangent of 0.025 is used as the system circuit board with ground plane on its back. It has a dimension of 155 mm × 75 mm × 0.8 mm, which is compatible with a 6.2-inch smartphone. Four metal-frames, including two long frames and two short frames, are arranged vertically around the FR4 substrate. All the four frames have the same height of 6 mm.
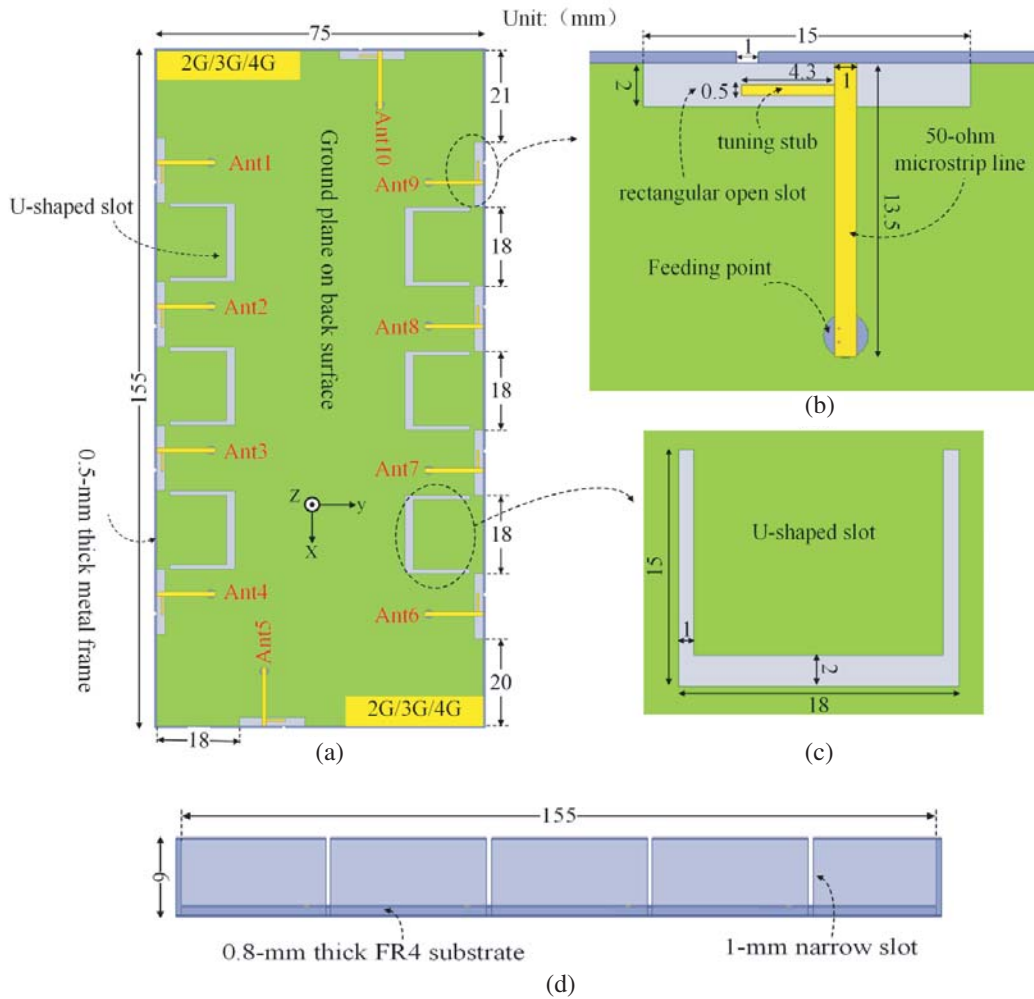
**Figure 1.** Geometry and dimensions of the proposed MIMO antenna array. (a) Overall structure. (b) Antenna element. (c) U-shaped decoupling structure. (d) Side view.

As shown in Figure 1(a), eight identical antenna elements are placed on the long side of the system circuit board, and the other two are placed on the short side. The purpose of this layout is to use spatial diversity techniques to reduce the mutual coupling between the short side antenna and long side antenna. At the same time, a U-shaped decoupling structure is also added to decrease the mutual coupling between the antenna elements. Moreover, there is enough space at two corners located along the short edges of the printed circuit board (PCB), which is reserved for 2G/3G/4G MIMO antenna array in order to cover more frequency bands in the future.
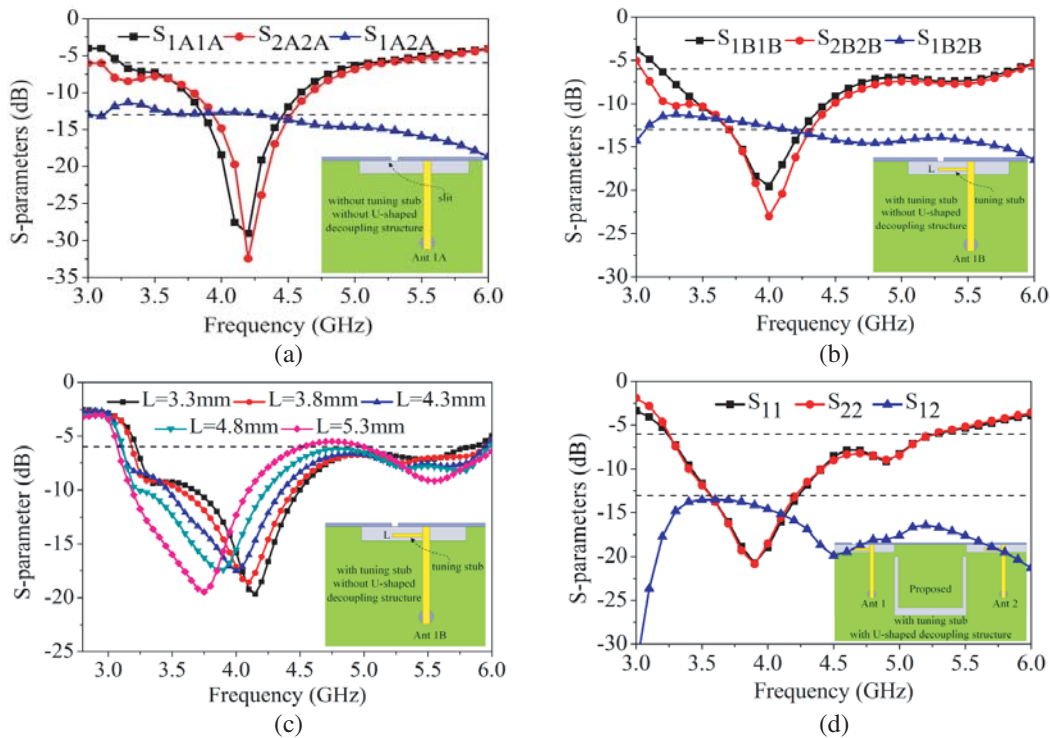
## 2.2. Antenna Element

By further observing the detailed geometry and dimensions of the antenna element illustrated in Figure 1(b), one can see that the element is formed by the 50-ohm microstrip feedline with a tuning stub. The microstrip feedline is connected to the side edge metal-frame, and a 1 mm wide slit on the metal-frame joins with the rectangular slot. As can be observed, the rectangular slot of size 15 mm × 2 mm is initially etched on the ground plane to provide better radiation performance of the multi-band antenna element. It is notable that the total width of the slot is merely 2 mm, indicating that the proposed antenna element has great advantage for narrow-frame smartphones. Decoupling technique becomes more critical but challengeable for designing MIMO antenna, as the number of antenna elements increases. Figure 1(c) shows the detailed structure of U-shaped decoupling. The size of the decoupling

structure is 15 mm × 1 mm, and the bottom edge is 18 mm × 2 mm. Figure 1(d) shows the side view of narrow slots on the metal-frame. The side-edge metal-frame is directly fed by the microstrip line, so part of it is exploited as the radiator to enhance the bandwidth. There will be a more detailed description of the impact of each part on the antenna performance in the next section.

## 2.3. Design Process

The design process of the proposed antenna is depicted in Figure 2. The metal-frame is considered as part of the antenna at the beginning of the design. As shown in Figure 2(a), in order to prevent the electromagnetic coupling caused by the metal-frame from deteriorating the radiation performance of the antenna array, a slit is cut on the metal frame in Ant1A. At the same time, in order to achieve omnidirectional radiation characteristics of antenna, a rectangular slot is etched on the ground plane. In this situation, the Ant1A excites a resonance mode around 4.2 GHz, and the bandwidth of the antenna is about 1500 MHz. Moreover, the isolation of the antenna in the low frequency band is relatively poor. The simulation results in Figure 2(a) show that its $S$-parameters cannot meet expectations.

In Figure 2(b), a tuning stub is added to change the bandwidth and center frequency by changing its length $L$. The tuning stub excites the resonance mode around 5.2 GHz, which greatly increases the antenna bandwidth to meet the design requirements; however, the isolation of the antenna in the low frequency band has not changed much. The variation of reflection coefficients with different values of length $L$ is shown in Figure 2(c). It can be clearly seen that the length $L$ affects the resonance frequency, as the value of length $L$ increases, and the resonant frequency of 4.0 GHz shifts towards low-frequency. On the contrary, the resonant frequency shifts to high-frequency. In Figure 2(d), the proposed antenna array and $S$ parameters are depicted, by adding a U-shaped slot to reduce the coupling between the antenna elements. It can be seen that after adding the decoupling structure, not only the isolation of the antenna in the low frequency band is improved, but also the isolation in the high frequency band is improved, and the bandwidth of the antenna is not reduced much. It shows that the U-shaped decoupling structure plays a great role in improving isolation. It can be found that the isolation between



**Figure 2.** Simulated $S$-parameter results of the different antenna structures. (a) Ant1A. (b) Ant1B. (c) Ant1B with different values of $L$. (d) Ant1 with U-shaped slot.

antenna elements Ant1 and Ant2 is much better than −13 dB. In summary, the structure and size of the antenna element are adjusted and optimized to meet the required performance of antenna array.

## 3. RESULTS AND DISCUSSION

The proposed 10-port MIMO antenna array was fabricated and measured, and its front and back views are demonstrated in Figure 3. The feeding strips of the proposed antenna element in the fabricated prototype are directly soldered to 50-ohm Sub-Miniature-A (SMA) connectors at the corresponding feed points for further measurements. In the following subsections, the proposed antenna array performances, including the $S$-parameters, radiation pattern, ECC, and user's hand effects, will be shown and discussed in detail. Because of the symmetric placements of the antenna elements, for brevity, only some measured parameters of Ant1 to Ant5 are given.



(a)          (b)
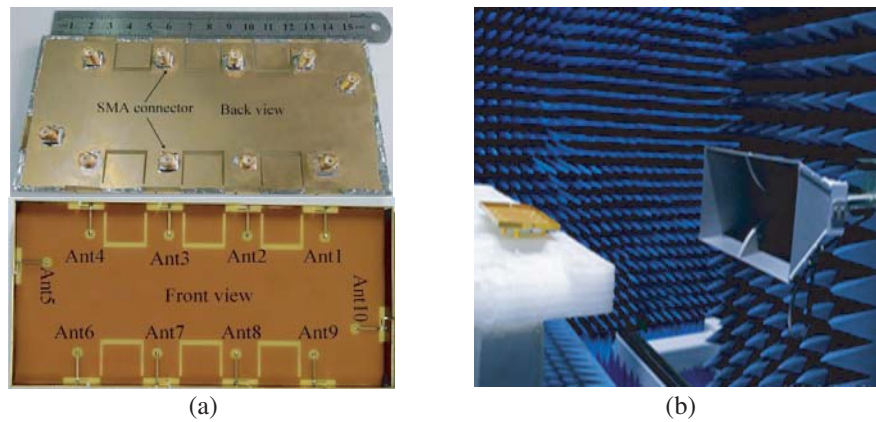
**Figure 3.** (a) Font and back view of the fabricated antenna array. (b) Microwave anechoic chamber.

### 3.1. $S$ Parameters

Simulated $S$-parameters of the proposed antenna elements are depicted in Figure 4. The $S$-parameters were measured with an Agilent N5247A vector network analyzer, and the corresponding results are given in Figure 5. It is observed that the measured $S$-parameters are well validated with the simulated ones.

It is clear that most antenna elements can completely cover the bandwidth of 3.3–5.5 GHz, with reflection coefficients less than −6 dB. However, the bandwidth of Ant3 and the resonance frequency of Ant4 are slightly different which may be caused by fabrication tolerance, connecter effect, and other
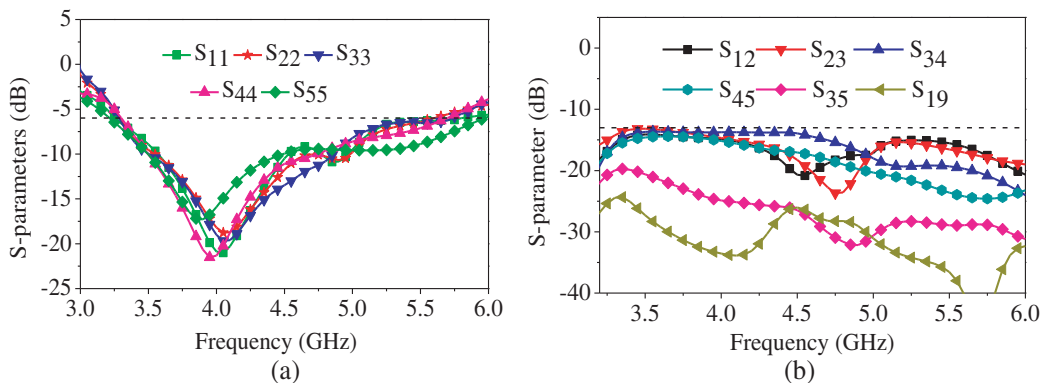


**Figure 4.** Simulated $S$-parameters. (a) Reflection coefficients. (b) Transmission coefficients.
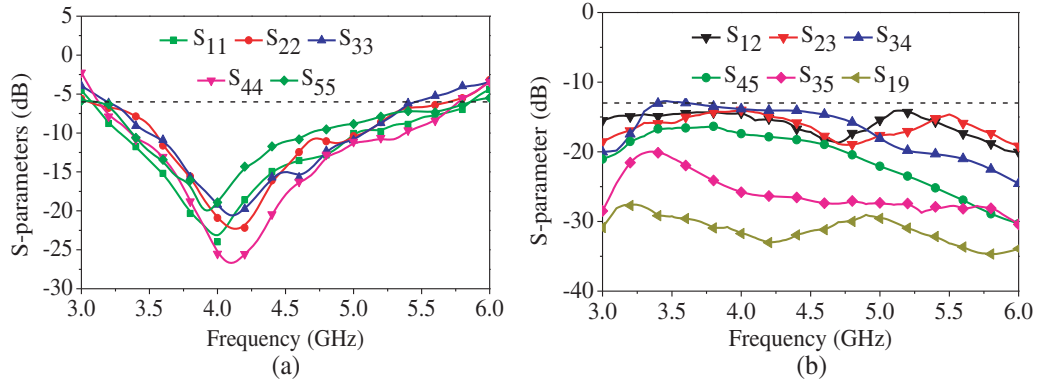
**Figure 5.** Measured $S$-parameters. (a) Reflection coefficients. (b) Transmission coefficients.

external factors. The measured transmission coefficients of some typical antenna pairs are shown in Figure 5(b). The transmission coefficients between the two adjacent antenna elements ($S_{12}$, $S_{23}$, $S_{34}$, and $S_{45}$) are better than $-13\,\text{dB}$. Due to farther layout distance, the isolation $S_{19}$ between Ant1 and Ant9 is better than $-25\,\text{dB}$. The measured and simulated results can validate each other well. The measured results show that within $3.3$–$5.5\,\text{GHz}$, the proposed MIMO antenna array can meet the performance requirements of both bandwidth and isolation.

## 3.2. Radiation Performances

The radiation performances of the proposed MIMO antenna array were measured in a microwave anechoic chamber. Because the antenna array elements are disposed symmetrically along the edges of the FR4 substrate, for brevity, only the results of the antenna elements Ant1, Ant3, and Ant5 are given. The radiation patterns in $xz$-plane and $yz$-plane of Ant1, Ant3, and Ant5 at $4.0\,\text{GHz}$ and $5.0\,\text{GHz}$ are plotted in Figure 6 and Figure 7, respectively. It can be clearly seen that the measured antenna elements have almost omnidirectional radiation characteristics in the $xz$ and $yz$ planes. Although there are low gain points in Figure 6(a), Figure 6(b), Figure 6(d), Figure 6(e), Figure 7(a), Figure 7(c), Figure 7(d), and Figure 7(f), the radiation performance of the antenna always has obvious complementarity in the phi direction or theta direction, which means that good pattern diversity characteristics are guaranteed.

In addition, the measured results of the antenna elements fluctuate to a certain extent compared with the simulation results in some directions. This is mainly due to errors caused by the test environment and some external disturbances, but the overall trends of the two results are similar. In short, these results indicate that the proposed antenna array has promising radiation performance in mobile communication applications.

## 3.3. MIMO Performances

Since the MIMO antenna array mainly works for diversity and multiplexing applications, besides reflection, isolation, and radiation performances, it is quite important to investigate the diversity and multiplexing performances. The ECC of diverse antenna pairs is studied in this subsection to evaluate the diversity performance of the proposed MIMO antenna array. Figure 8 shows that the calculated ECC values are lower than 0.06 in the $3.3$–$5.5\,\text{GHz}$, which is much better than the acceptable criterion of ECC less than 0.5. The results show that the proposed antenna array exhibits desirable MIMO diversity performance for 5G system. To verify the multiplexing performances under high signal-to-noise ratio (SNR) and also to figure out the data transmitting rate potential of the proposed MIMO antenna system under specific propagation scenario, the ergodic channel capacity is therefore studied here. The ergodic channel capacity C can be expressed as follows:
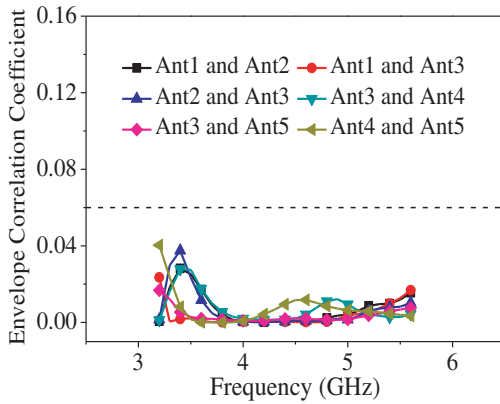
$$\text{C} = \text{E}\left\{\log_2\left[det\left(\mathbf{I}_M + \frac{SNR}{M}\mathbf{H}\mathbf{H}^H\right)\right]\right\} \tag{1}$$
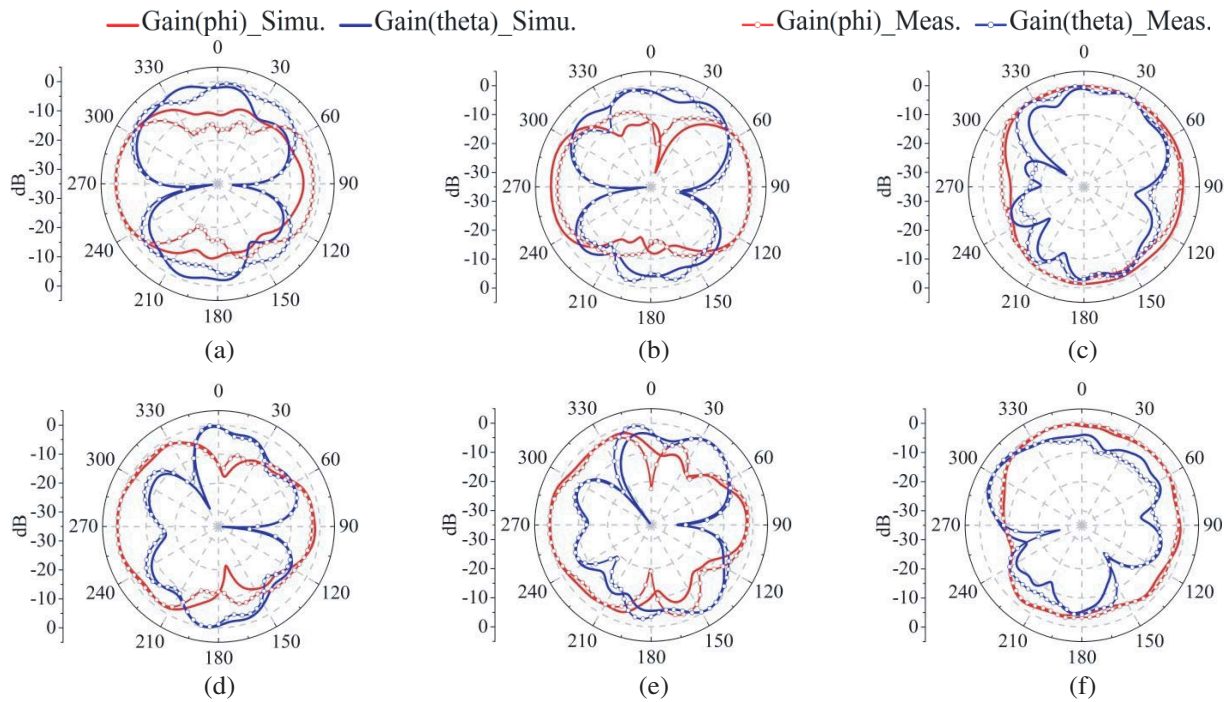
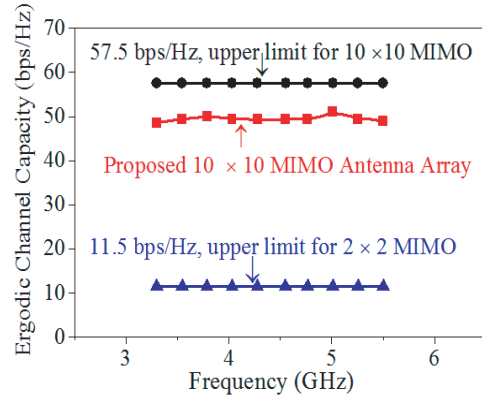**Figure 6.** Simulated and measured radiation patterns in $xz$-plane. (a) Ant1. (b) Ant3. (c) Ant5 at 4.0 GHz. (d) Ant1. (e) Ant3. (f) Ant5 at 5.0 GHz.
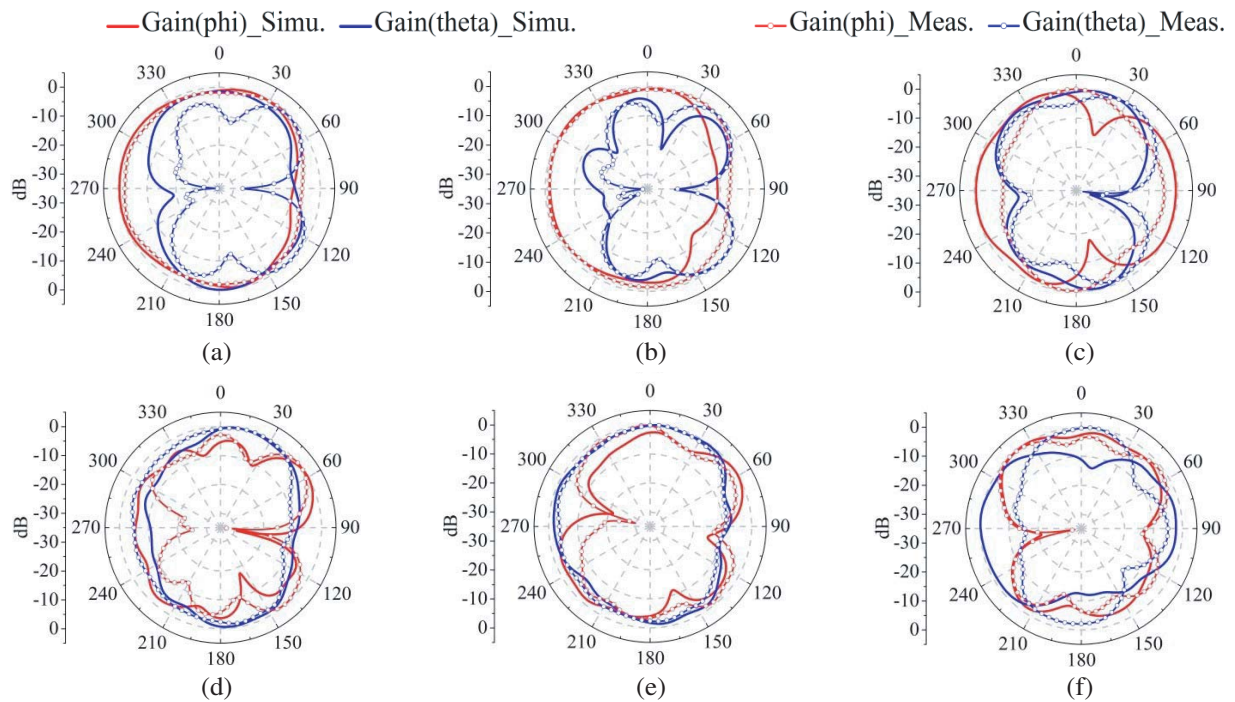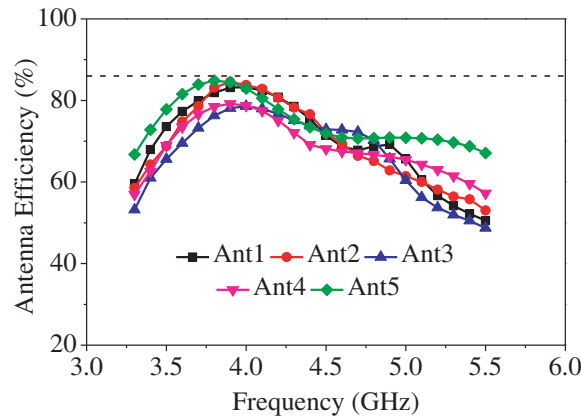


**Figure 7.** Simulated and measured radiation patterns in $yz$-plane. (a) Ant1. (b) Ant3. (b) Ant5 at 4.0 GHz. (d) Ant1. (e) Ant3. (f) Ant5 at 5.0 GHz.

**Figure 8.** Simulated ECCs between some adjacent antenna elements.



**Figure 9.** Calculated ergodic channel capacity of the proposed antenna array.



**Figure 10.** Simulated antenna efficiencies of Ant1 to Ant5.

As shown in Equation (1), $E(\cdot)$ denotes the expectation with respect to diverse MIMO channel realizations; $\mathbf{I}_M$ is a $M \times M$ identity matrix; SNR is signal-to-noise ratio at the receiver; $\mathbf{H}$ is the channel matrix; and $(\cdot)^H$ denotes the Hermitian transpose. The ergodic channel capacity of the proposed antenna array is calculated, as shown in Figure 9, by assuming that the MIMO system is in an independent and identically distributed Rayleigh fading environment with the SNR of 20 dB. Here, the ten transmitting antennas are assumed to be uncorrelated (correlation coefficient $= 0$) and lossless (total efficiency $= 100\%$), whereas the ten antenna elements of the proposed antenna array serve as the receiving antennas. It can be seen from Figure 9 that in the range of 3.3–5.5 GHz, the ergodic channel capacities of the proposed antenna array operating at $10 \times 10$ MIMO scheme are about 49–51 bps/Hz, which is about 4.35 times higher than the upper limit (11.5 bps/Hz) of traditional $2 \times 2$ MIMO system in the same propagation environment. Therefore, the proposed 10-port MIMO antenna array also possesses strong spatial multiplexing capability.

Figure 10 shows the simulated antenna efficiencies of Ant1 to Ant5. As can be seen from the graph, the efficiency of Ant1 to Ant4 is lower than that of Ant5, because of higher coupling losses between the adjacent antenna elements. In general, the obtained antenna efficiencies are about 46%–83% within the entire bandwidth, which are desirable for achieving low capacity loss.

## 3.4. User's Hand Effects and SAR

For the design of smartphone antenna, it is indispensable to consider the effect of user's hand posture on the antenna performances. At the same time, the specific absorption rate (SAR) effect of the smartphone

antenna on the human head is also very important in practical applications. In this section, some key parameters will be briefly investigated using HFSS software.

Figure 11 shows the corresponding changes of all elements' bandwidth performances of the proposed $10 \times 10$ MIMO antenna array under right hand holding posture. As depicted in Figure 11(a), the bandwidth of some elements which are in direct contact with the hand phantom will be slightly deviated, such as Ant1, Ant2, and Ant3. In Figure 11(b), it can be seen that the user's hand has a great impact on the antenna, so that the bandwidth of some antenna elements cannot cover 3.3–3.6 GHz, such as Ant8, Ant9, and Ant10, whereas the 10-port MIMO antenna elements are placed in different positions, and the user's holding posture does not touch all the antenna elements, so there are still some antenna elements that are not affected due to the distance away from the user's hand, such as Ant4, Ant5, and Ant6. It can be obviously known from simulated results that the array performances are closely related to the distance between antenna element and the hand. The closer the distance is, the greater the impact will be on the bandwidth and performances.
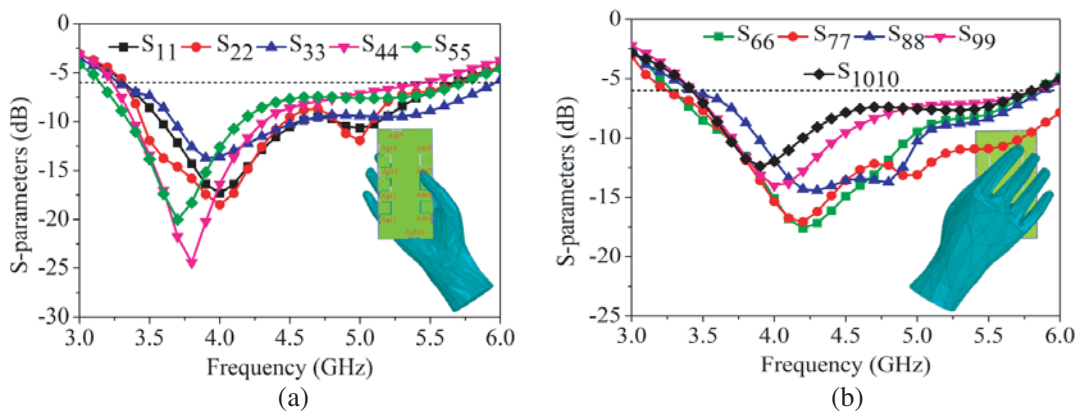


**Figure 11.** Simulated $S$-parameters with single-hand holding: (a) Reflection coefficients for Ant1 to Ant5, (b) reflection coefficients for Ant6 to Ant10.

SAR refers to the electromagnetic radiation energy absorbed by a unit of mass per unit time. Its value is usually used to measure the thermal effect of terminal radiation, which is a critical issue for smartphone systems and should be as low as possible. It should be noted that the distance between MIMO antenna and the human-head has important influence on the SAR values. The smartphone is placed as shown in Figure 12, and the simulation results show that the average value of the SAR obtained is less than the internationally specified upper limit of 1.6 w/kg, which meets the design requirements and is consistent with the actual application.
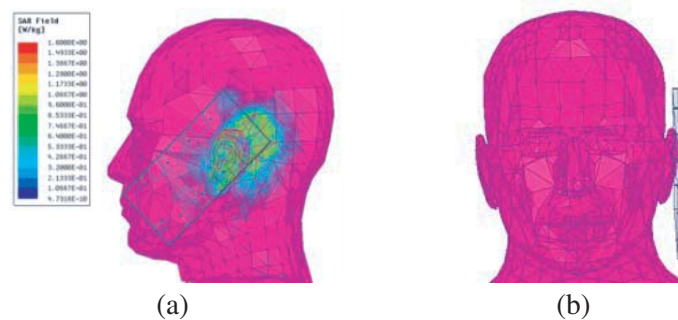


**Figure 12.** SAR of the proposed antenna element Ant1 at 4.0 GHz. (a) Front view. (b) Side view.

**Table 2.** Comparison with other previously published antennas.

| Reference | Metal Frame | Dimension (mm$^3$) | Bandwidth (GHz) | Efficiency (%) | Isolation (dB) | ECC | Peak Channel Capacity (20 dB SNR) |
|---|---|---|---|---|---|---|---|
| **Proposed** | **With** | **155 × 75 × 0.8** | **3.3–5.5** | **46–83** | **> 13** | **< 0.06** | **49 bps/Hz** **(10 × 10)** |
| [3] | Without | 150 × 75 × 1.6 | 3.4–3.8 | 60–80 | > 15 | < 0.5 | Not given (8 × 8) |
| [4] | Without | 140 × 70 × 0.8 | 3.4–3.8 | 38–62 | > 10 | < 0.1 | 47 bps/Hz (8 × 8) |
| [7] | Without | 150 × 75 × 0.8 | 3.4–3.6 | 50–75 | > 12.5 | < 0.2 | 57 bps/Hz (12 × 12) |
| [9] | With | 150 × 75 × 0.8 | 3.3–5.925 | 40–71 | > 11 | < 0.1 | 40 bps/Hz (8 × 8) |
| [10] | With | 155 × 75 × 0.8 | 3.4–3.6 | 42–75 | > 13 | < 0.15 | Not given (8 × 8) |
| [11] | Without | 150 × 80 × 0.8 | 3.4–3.8 5.15–5.925 | 42–65 62–82 | > 11 | < 0.15 < 0.05 | 48 bps/Hz (10 × 10) |
| [12] | Without | 150 × 75 × 0.8 | 3.4–3.6 4.8–5.1 | 40–85 | > 11.5 | < 0.08 < 0.05 | 38.5 bps/Hz (8 × 8) |
| [18] | Without | 150 × 75 × 0.8 | 3.3–4.2 4.8–5.0 | 53–76 62–79 | > 12.5 | < 0.1 < 0.12 | 40 bps/Hz (8 × 8) |
| [19] | Without | 136 × 68 × 0.8 | 3.4–3.6 | 40–60 | > 10 | < 0.2 | 36.5 bps/Hz (8 × 8) |
| [21] | With | 150 × 75 × 0.8 | 2.496–2.69 3.4–3.8 | 48–66 44–59 | > 10.5 > 11 | < 0.2 < 0.05 | 38.3 bps/Hz (8 × 8) |

## 4. CONCLUSION

A wideband 10-port MIMO antenna array which can completely cover 3.3–5.5 GHz for 5G metal-frame smartphones is presented in this paper. The isolations, better than −13 dB, are achieved by a decoupling structure between the two adjacent antenna elements. Any two antenna elements in the proposed array also show good ECC of less than 0.06. The antenna efficiencies of the antenna element are higher than 46% in the operating band. Meanwhile, the calculated channel capacity of the 10-port MIMO antenna array is about 49 bps/Hz with 20 dB SNR for the desired band, which is at least 4.3 times larger than the upper limit for an ideal 2 × 2 MIMO system. Furthermore, the proposed antenna array is resistant to effects of single-hand operations in practical usage scenarios. Table 2 exhibits the comprehensive comparison of the proposed MIMO antenna array and the referenced 5G smartphones reported in the last few years. Apparently, the proposed 10-antenna array can be successfully integrated with metal frames, which is a unique feature that most of the referential works do not possess. Compared with other MIMO antenna arrays, due to good performances in bandwidth, isolation, efficiency, channel capacity, and SAR values, the proposed MIMO antenna array has a broad prospect for 5G metal-frame smartphones.

## ACKNOWLEDGMENT

# REFERENCES

1. Hong, W., "Solving the 5G mobile antenna puzzle: Assessing future directions for the 5G mobile antenna paradigm shift," *IEEE Microwave Magazine*, Vol. 18, No. 7, 86–102, 2017.

2. Al-Dulaimi, Z., T. A. Elwi, and D. C. Atilla, "Design of a meander line monopole antenna array based hilbert-shaped reject band structure for MIMO applications," *IETE Journal of Research*, Vol. 66, 1–10, 2020.

3. Elwi, T. A., M. Noori, Y. Al-Naiemy, and E. S. Yahiea, "Conformal antenna array for MIMO applications," *Journal of Electromagnetic Analysis and Applications*, Vol. 6, No. 4, 43–50, 2014.

4. Alsaif, H., M. Usman, M. T. Chughtai, and J. Nasir, "Cross polarized $2 \times 2$ UWB-MIMO antenna system for 5G wireless applications," *Progress In Electromagnetics Research M*, Vol. 76, 157–166, 2018.

5. Parchin, N. O., et al., "Eight-element dual-polarized MIMO slot antenna system for 5G smartphone applications," *IEEE Access*, Vol. 7, 15612–15622, 2019.

6. Wong, K. L. and J. Y. Lu, "3.6 GHz 10-antenna array for MIMO operation in the smartphone," *Microwave and Optical Technology Letters*, Vol. 57, No. 7, 1699–1704, 2015.

7. Yang, M. and J. Zhou, "A broadband high-Isolation dual-polarized antenna for 5G application," *Progress In Electromagnetics Research M*, Vol. 85, 39–48, 2019.

8. Wong, K. L., C. Y. Tsai, and J. Y. Lu, "Two asymmetrically mirrored gap-coupled loop antennas as a compact building block for eight-antenna MIMO array in the future smartphone," *IEEE Transactions on Antennas and Propagation*, Vol. 65, No. 4, 1765–1778, 2017.

9. Li, M. Y., Y. L. Ban, Z. Q. Xu, J. Guo, and Z. F. Yu, "Tri-polarized 12-antenna MIMO array for future 5G smartphone applications," *IEEE Access*, Vol. 6, 6160–6170, 2017.

10. Swain, B. R. and A. K. Sharma, "An investigation of dual-band dual-squarering (DSR) based microstrip antenna for WiFi/WLAN and 5G-NR wireless applications," *Progress In Electromagnetics Research M*, Vol. 86, 17–26, 2019.

11. Zhang, X., Y. Li, W. Wang, and W. Shen, "Ultra-wideband 8-port MIMO antenna array for 5G metal-Frame smartphones," *IEEE Access*, Vol. 7, 72273–72282, 2019.

12. Huang, D., Z. Du, and Y. Wang, "Slot antenna array for fifth generation metal frame mobile phone applications," *Int. J. RF Microw. Comput. Aided Eng.*, Vol. 29, No. 7, 1–9, 2019.

13. Li, Y., C. Sim, Y. Luo, and G. Yang, "Multiband 10-antenna array for sub-6 GHz MIMO applications in 5G smartphones," *IEEE Access*, Vol. 6, 28041–28053, 2018.

14. Guo, J. L., L. Cui, C. Li, and B. H. Sun, "Side-edge frame printed eight-port dual-band antenna array for 5G smartphone applications," *IEEE Trans. Antennas Propag.*, Vol. 66, No. 12, 7412–7417, 2018.

15. Stanley, M., Y. Huang, H. Wang, H. Zhou, Z. Tian, and Q. Xu, "A novel reconfigurable metal Rim integrated open slot antenna for octa-band smartphone applications," *IEEE Transactions on Antennas and Propagation*, Vol. 65, No. 7, 3352–3363, 2017.

16. Zhao, X., S. P. Yeo, and L. C. Ong, "Decoupling of inverted-F antennas with high-order modes of ground plane for 5G Mobile MIMO platform," *IEEE Transactions on Antennas and Propagation*, Vol. 66, No. 9, 4485–4495, 2018.

17. Siu, L., H. Wong, and K. M. Luk, "Self-decoupled compact metal-frame LTE MIMO antennas for the smartphone," *Microwave and Optical Technology Letters*, Vol. 60, 1170–1179, 2018.

18. Kurvinen, J., A. Lehtovuori, J. Mai, C. Wang, and V. Viikari, "Metal-covered handset with LTE MIMO, Wi-Fi MIMO, and GPS antennas," *Progress In Electromagnetics Research C*, Vol. 80, 89–101, 2018.

19. Arvind, K., C. Divya, and R. Singaravelu, "Design of a Self-Diplexing Antenna Using SIW Technique with High Isolation," *AEU — International Journal of Electronics and Communications*, Vol. 94, 386–391, 2018.

20. Kumar, A., D. Chaturvedi, M. Saravanakumar, et al., "SIW cavity-backed self-triplexing antenna with T-shaped slot," *Asia-Pacific Microwave Conferenc (APMC)*, No. 6, 1588–1590, 2018.

21. Alnaiemy, Y., T. A. Elwi, and L. Nagy, "Mutual coupling reduction in patch antenna array based on EBG structure for MIMO applications," *Periodica Polytechnica Electrical Engineering and Computer Science*, Vol. 1, No. 4, 1–11, 2019.

22. Wong, K. L., B. W. Lin, and W. Y. Li, "Dual-band dual inverted-F/loop antennas as a compact decoupled building block for forming eight 3.5/5.8-GHz MIMO antennas in the future smartphone," *Microwave and Optical Technology Letters*, Vol. 59, No. 11, 2715–2721, 2017.

23. Cui, L., J. Guo, Y. Liu, and C. Sim, "An 8-element dual-band MIMO antenna with decoupling stub for 5G smartphone applications," *IEEE Antennas and Wireless Propagation Letters*, Vol. 18, No. 10, 2095–2099, 2019.

24. Abdullah, M., Y.-L. Ban, K. Kang, M.-Y. Li, and M. Amin, "Eight-element antenna array at 3.5 GHz for MIMO wireless application," *Progress In Electromagnetics Research C*, Vol. 78, 209–216, 2017.

25. Ren, A., Y. Liu, and C. Sim, "A compact building block with two shared-aperture antennas for eight-antenna MIMO array in metal-rimmed smartphone," *IEEE Transactions on Antennas and Propagation*, Vol. 67, No. 10, 6430–6438, 2019.

26. Li, Y. D., C. Y. Sim, et al., "Metal-frame-integrated eight-element multiple-input multiple-output antenna array in the long term evolution bands 41/42/43 for fifth generation smartphones," *International Journal of RF and Microwave Computer-Aided Engineering*, Vol. 29, No. 1, 1170–1179, 2018.

27. Chen, Q., et al., "Single ring slot-based antennas for metal-rimmed 4G/5G smartphones," *IEEE Transactions on Antennas and Propagation*, Vol. 67, No. 3, 1476–1487, 2019.